VIII. COMMUNICATIONS RESEARCH

A. MULTIPATH TRANSMISSION

Prof. L. B. Arguimbau
B. Brown
J. Granlund
W. L. Hatton
R. A. Paananen

1. Speech and Music

a. Theory

In the past quarterly period, the heuristic expression for rms interference given in the Progress Report, April 15, 1949 was considered in more detail. A rigorous justification was found for this expression and also for a simpler, allied problem.

The allied problem is the computation of the power spectrum of a transmitter with sinusoidal frequency modulation. When the problem is handled in a conventional mathematical way there is no formal difficulty. However, if we take the point of view that we are observing the spectrum with a sharply tuned wave analyzer, the "answer" seems obvious. Since the total power emitted is constant, the power in a narrow frequency range $\Delta\omega$ is simply the total power multiplied by the probability that the frequency lies in the range $\Delta\omega$ under consideration. This gives rise to a continuous spectrum having infinite peaks at the ends of the frequency excursion, and is perhaps more familiar as the amplitude probability distribution of a sine wave. These considerations are not limited to modulating wave shape; in fact, they may be applied to random modulation.

The above "answer", in spite of its plausibility, is of course correct in a limiting sense only. The difficulty can be explained in terms of the wave analyzer used to measure the spectrum. If the instantaneous frequency of the transmitter moves rapidly across the narrow wave-analyzer pass band, the measuring equipment will be subjected to a series of long transients with a duration of the order of $1/\Delta\omega$. The average power in these transients need not bear any resemblance to the transmitter power multiplied by the fraction of time that the frequency lies in $\Delta\omega$. Thus it is not surprising to find that the spectrum in the case of sinusoidal modulation is a line spectrum. However, if the modulation frequency is reduced, the lines increase in number and get closer together. By means of a suitable limiting process, we have been able to show that the line spectrum approaches the continuous spectrum described above.

Practically it is necessary only that the modulating frequency be small compared with the frequency swing and with the bandwidths of the circuits

used. In other words, we are not interested in the fine structure of the spectrum, and the energy distribution predicted on the static basis is a reasonable approximation for wide-band frequency modulation.

The calculation of the audio interference resulting from the reception of two frequency-modulated signals is similar to the problem just considered. Finding the audio power spectrum of the interference after detection, but before audio filtering, is the major part of this calculation. The detected audio output (for a discriminator with unit slope) differs from the output due to the stronger signal alone by

$$\Delta p = \frac{d}{dt}\left(\tan^{-1}\frac{a \sin\theta}{1 + a\cos\theta}\right) = -\frac{d\theta}{dt}\sum_{n=1}^{\infty}(-a)^n \cos n\theta \ldots \quad (1)$$

where a is the ratio of the weaker to the stronger signal, and θ is the phase difference between weaker and stronger signals. $d\theta/dt$ is the instantaneous frequency difference between weaker and stronger signals, and is not assumed to be constant, or even to have sinusoidal variation with time.

If we regard each term of the above summation as a wave that is simultaneously amplitude- and frequency-modulated, we might argue as before that the power in a narrow frequency range, $\Delta\omega$, is

$$\sum_{n=1}^{\infty}\frac{1}{2}\left(a^n\frac{d\theta}{dt}\right)^2 \times (\text{probability that } n\frac{d\theta}{dt} \text{ lies in } \Delta\omega) \ldots \quad (2)$$

As in the previous problem, the case of sinusoidal variation of frequency difference has been studied in detail. In this case we have shown that the power spectrum approaches the sum of the continuous spectra of the terms of Eq. (1), computed on this static basis, as the ratio of modulating frequency to peak frequency difference approaches zero. J. Granlund

b. Limiter design

In the course of the design of a second laboratory receiver an attempt was made to gain a better insight into the operation of a fast-acting limiter employing germanium crystals. To this end a set of E-I curves for a 1N34 crystal (Fig. VIII-2) was experimentally obtained at a low frequency (60 cycles) with the expectation that they would be accurate up to 60 Mc, for example.

Figure VIII-1 shows a typical limiter stage with C as the distributed capacity of the tubes and wiring. As a first approximation it may be assumed that the voltage across the tank circuit, and hence the crystals, is sinusoidal. Also I_c is merely the fundamental component of I since the tank

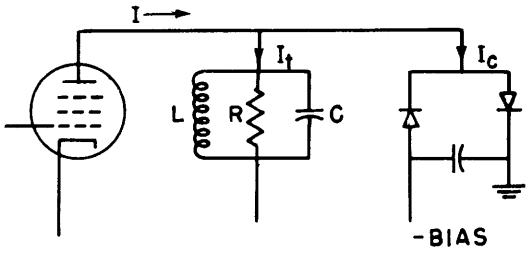

Fig. VIII-1 Typical limiter stage.

circuit is a low impedance to harmonic components. Therefore the behavior of this circuit can be predicted by measuring the fundamental component of current through the crystals with a sine wave of some conveniently low frequency applied. This results in the curves of Fig. VIII-2.

The 6000-ohm line in this figure represents a possible impedance of the tank circuit at resonance. Then, since the tube current is equal to the sum of the tank and crystal currents, these two currents can be added for any tank voltage and a composite curve obtained as in Fig. VIII-3.

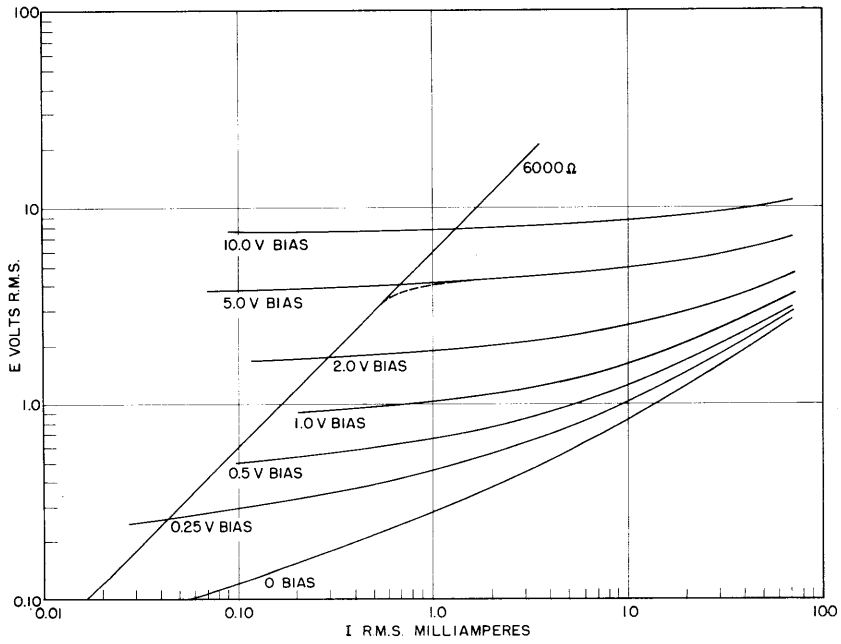

Fig. VIII-2 Current-voltage characteristics of a pair of IN34 crystals as a function of bias.

Or we can look at it in another way. If the tube current is not enough to make the crystals conduct, the operation is as a linear amplifier along the 6000-ohm line, shifting to the nearly flat region for larger drives.

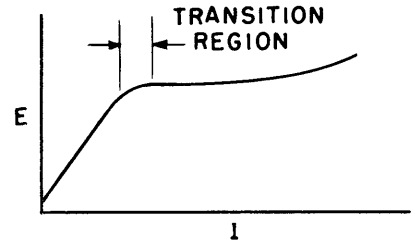

Fig. VIII-3 Typical composite curve.

Thus for any input voltage we can calculate the tube current easily and hence obtain the sinusoidal output voltage from the composite curve. For operation at frequencies off resonance a new impedance line can be drawn corresponding to the impedance of the tank circuit at that frequency.

The curves have been checked quite closely at 28 Mc with most of the disagreement attributable to grid-plate capacity of the tube and to detuning of the tank circuit by the variable loading of the crystals.

R. A. Paananen

c. Three-path multipath interference

Theoretical and experimental work on the effect of three simultaneous signals has been started.

B. Brown

2. Television

An investigation is being made into the possibility of using pre-emphasis in television in conjunction with frequency modulation. In audio FM systems the interference reduction is proportional to the ratio of the pre-emphasis turn-over frequency to the maximum deviation. In this case, the turn-over frequency is under 2 kc, and the deviation is 75 kc, giving a suppression of about 37 to 1 of the interference. It is not expected that such a large interference suppression ratio can be attained in a practical television system.

The difficulty comes in the increase in peak video level that occurs after pre-emphasis. In the audio case, the peak level is increased approximately 1 db with the present standards. A video signal, however, contains a great number of transitions in level which occur at the maximum speed of the system. When one of these transitions is passed through the pre-emphasis network, an overshoot occurs which may be of considerable magnitude.

A number of these overshoots have been calculated graphically for a typical transition. The pre-emphasis network used was not the idealized one whose output continues to rise at 6 db per octave from the turn-over frequency to infinity, but the more practical network whose output rises from the turn-over frequency to some other frequency where it levels off. For realistic results, the upper frequency should be above the cut-off of the other amplifiers in the circuit. The pre-emphasis transfer function is then

$$K \frac{1 + T_1 s}{1 + T_2 s} .$$

Here K is a constant, T_1 is the turnover time constant, T_2 is the time constant associated with the upper limiting frequency, and s is the complex frequency variable. The results are plotted as a function of T_1 and $R = T_2/T_1$ in Fig. VIII-4.

It can be seen that if the transition before pre-emphasis represents

an appreciable portion of the total range from white to black, the peak value of the video signal will be greatly increased. The question then arises as to what can be done about these large values. One possibility

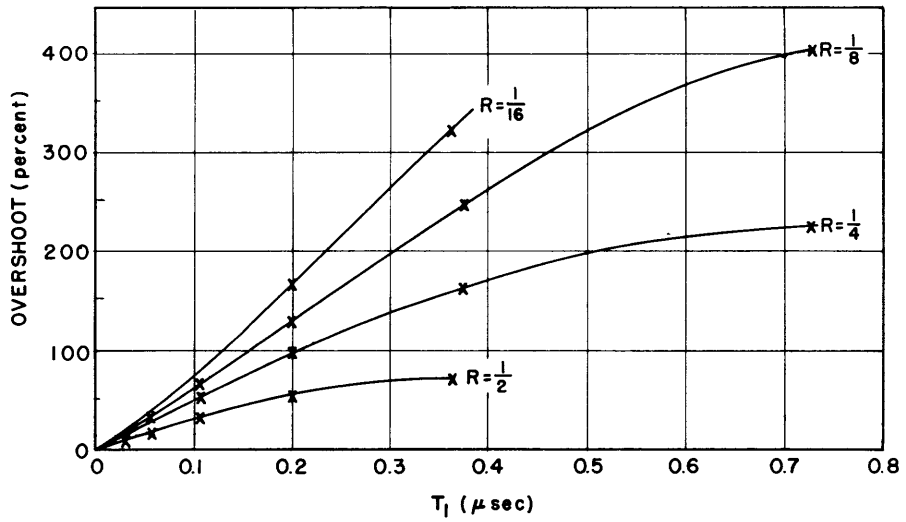

Fig. VIII-4 Overshoot due to pre-emphasis.

is to clip off peaks which exceed a certain fixed level, and hope that after de-emphasis, not too much deterioration in waveshape will result. It can be seen that the transitions that are most affected are those from full white to full black, and that transitions between intermediate grays will not be affected at all. Calculations have been carried out for a few cases of the resulting waveforms after clipping and de-emphasis, and this work is continuing.

The problem of generating a wide-deviation FM signal is also under consideration. The present attempt to solve the problem is to use two klystrons operating at about 10,000 Mc with a difference of 200 Mc and beating their outputs together in a crystal. Each klystron can be deviated electronically about 40 Mc so it should be possible to achieve signals at 200 Mc deviated by 20 Mc on each side. The klystrons used for this application are 2K39's in Mk. SX12 power supplies. The two outputs are combined in a "magic tee" with crystals in the other two arms. W. L. Hatton

B. STATISTICAL THEORY OF COMMUNICATION

Prof. J. B. Wiesner	E. H. Gibbons
Prof. W. B. Davenport, Jr.	P. E. Green, Jr.
Prof. R. M. Fano	L. G. Kraft
Prof. Y. W. Lee	A. J. Lephakis
P. E. A. Cowley	L. Levine
E. E. David, Jr.	H. E. Singleton
L. Dolansky	O. H. Straus
J. Fairfield, Jr.	C. A. Stutt

1. Digital Electronic Correlator

A report on this correlator is being prepared. At present the machine is being tested. A sample result of the testing is shown in Fig. VIII-5.

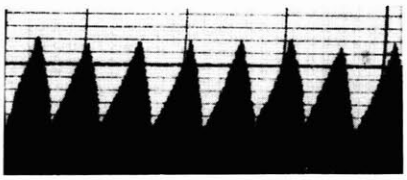

Fig. VIII-5 Autocorrelation function of a square wave.

The sawtooth wave is the autocorrelation function of a square wave.

Y. W. Lee, H. E. Singleton, L. G. Kraft

2. Detection of Small Signals in Noise

The theory of detection of small periodic signals in noise through use of autocorrelation and crosscorrelation functions has been extended so that not only the presence of a periodic function but its actual waveform may be detected. This is accomplished by crosscorrelating the signal and noise with a periodic unit impulse function. The theory has been roughly checked with the electronic correlator. A circuit is being designed for the special type of crosscorrelation required in the signal waveform detection.

Y. W. Lee, L. G. Kraft

3. Crosscorrelation Demonstrator

The use of crosscorrelation for detection of a sinusoid in noise has been demonstrated by a simple device in which signal and noise are crosscorrelated with a square wave. It has been possible to achieve a considerable improvement in signal-to-noise voltage ratio. Similar results were obtained previously by J. C. R. Licklider of the Harvard Psycho-Acoustic

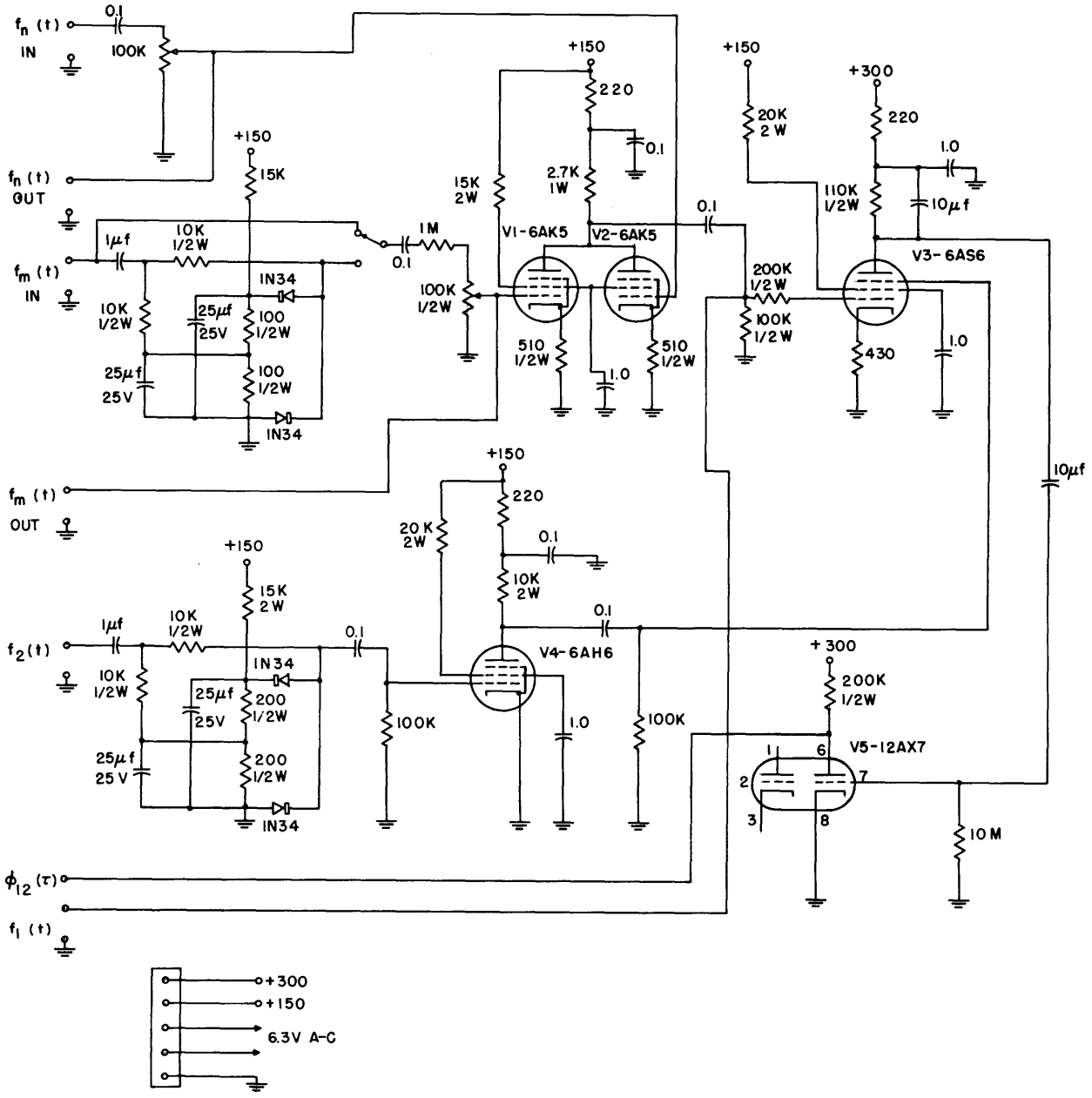

Fig. VIII-6 Circuit diagram of crosscorrelation demonstrator.

Laboratory with a somewhat different circuit.

Figure VIII-6 is a circuit diagram of the demonstrator. Typical values of inputs used with this device are: $f_m(t)$ is a 1000-cps sinusoid of 0.005 volts rms amplitude, $f_n(t)$ is a random noise of approximately 200-kc bandwidth and 0.5 volt rms amplitude, $f_2(t)$ is a sinusoid of about 35 volts rms amplitude which is shaped into a square wave of about 20 volts peak-to-peak amplitude at the grid of V3. (The frequency of $f_2(t)$ is the same as that of $f_m(t)$, but $f_2(t)$ is made to shift phase with respect to $f_m(t)$ at approximately one cycle per second.) An Esterline-Angus recording ammeter was used to plot the output, $\phi_{12}(t)$, continuously. A sample of the output curve is shown in Fig. VIII-7. For the first part of the sample $f_m(t)$ was zero. In the latter part $f_m(t)$ was 0.005 volts rms.

J. B. Wiesner, H. E. Singleton

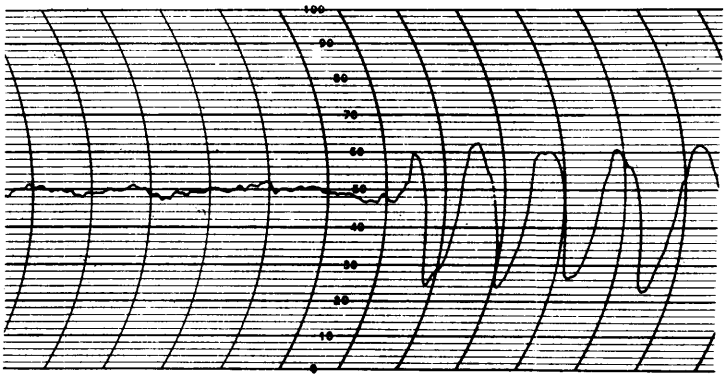

Fig. VIII-7 Crosscorrelation function showing detection of a small sinusoid in noise.

4. Experimental Determination of System Functions by the Method of Correlation

A mathematical analysis of this problem has been made showing that if a stationary random function is applied to a linear system, the input autocorrelation function $\phi_{ii}(\tau)$, the input-output crosscorrelation function $\phi_{io}(\tau)$ and the system unit-impulse response characteristic h(t) are related by the convolution integral

$$\phi_{io}(\tau) = \int_{-\infty}^{\infty} h(t)\ \phi_{ii}(\tau - t)dt \quad . \tag{1}$$

The corresponding relation in the frequency domain is

$$\Phi_{io}(\omega) = H(\omega)\ \Phi_{ii}(\omega) \tag{2}$$

where $\Phi_{io}(\omega)$ is the cross-power density spectrum between the input and

output, $\Phi_{ii}(\omega)$ the power density spectrum of the input and $H(\omega)$ the system transfer function. The power density spectrum is the Fourier transform of the correlation function.

If the input is a white noise with the spectrum $\Phi_{ii}(\omega) = 1/2\pi$, the integral (1) reduces to

$$\phi_{io}(\tau) = h(\tau) \quad . \tag{3}$$

This result states that for a linear system with a white noise source, the crosscorrelation function between input and output is identical in form with the unit-impulse response characteristic of the system. Eq. (3) in the frequency domain is

$$H(\omega) = 2\pi \Phi_{io}(\omega) \quad . \tag{4}$$

As soon as the digital electronic correlator is ready for use, application of this theory will be made in the determination of system characteristics with a white noise source.

When the amplitude of the system function alone is of primary interest, the following known relation will be useful:

$$\Phi_{oo}(\omega) = \left|H(\omega)\right|^2 \Phi_{ii}(\omega) \quad . \tag{5}$$

Here $\Phi_{oo}(\omega)$ is the output power density spectrum. In the case of a white noise source, the amplitude characteristic of the system function is

$$\left|H(\omega)\right| = \sqrt{2\pi \Phi_{oo}(\omega)} \quad . \tag{6}$$

Y. W. Lee

5. Optimum Linear System Design Criteria

Wiener's criterion in linear system design is the minimum-mean-square-error criterion. The mean square error $\mathcal{E}$ in a general form is

$$\mathcal{E} = \lim_{T\to\infty} \frac{1}{2T} \int_{-T}^{T} \left[f_o(t) - f_d(t)\right]^2 dt \tag{1}$$

in which $f_o(t)$ is the actual output and $f_d(t)$ is the desired output. These functions are of the stationary random type. The minimization of $\mathcal{E}$ leads to the Wiener-Hopf equation

$$\phi_{id}(\tau) = \int_{-\infty}^{\infty} h(\sigma)\phi_{ii}(\tau - \sigma)d\sigma \qquad \text{for } \tau \geqslant 0 \tag{2}$$

from which the unit-impulse response characteristic h(t) of the optimum

system is obtained. Here $\phi_{id}(\tau)$ is the input-desired output crosscorrelation function and $\phi_{ii}(\tau)$ is the autocorrelation function of the input.

A modification of the Wiener criterion is obtained by considering the integral square of the difference between the input-actual output crosscorrelation function $\phi_{io}(\tau)$ and the input-desired output crosscorrelation function. Thus the integral square error of the crosscorrelation function $\phi_{io}(\tau)$ is

$$\mathcal{E}_{\phi} = \int_{-\infty}^{\infty} \left[\phi_{io}(\tau) - \phi_{id}(\tau)\right]^2 d\tau \quad . \tag{3}$$

Analysis shows that the minimization of this error leads to an integral equation of the Wiener-Hopf type which is

$$\phi_{ii-id}(\tau) = \int_{-\infty}^{\infty} h(\sigma)\phi_{ii-ii}(\tau - \sigma)d\sigma \qquad \text{for } \tau \geqslant 0 \quad . \tag{4}$$

Here the double correlation functions $\phi_{ii-id}(\tau)$ and $\phi_{ii-ii}(\tau)$ are

$$\phi_{ii-id}(\tau) = \int_{-\infty}^{\infty} \phi_{ii}(t)\phi_{id}(t + \tau)dt \tag{5}$$

and

$$\phi_{ii-ii}(\tau) = \int_{-\infty}^{\infty} \phi_{ii}(t)\phi_{ii}(t + \tau)dt \quad . \tag{6}$$

The solution of Eq. (4) may be written according to the solution of Eq. (2) which is known.

Another modification of the measure of error is the weighted integral square correlation error

$$\mathcal{E}_{w\phi} = \int_{-\infty}^{\infty} w(\tau) \left[\phi_{io}(\tau) - \phi_{id}(\tau)\right]^2 dt \quad . \tag{7}$$

One form of the weighting function $w(\tau)$ may be $e^{-a^2\tau^2}$. A similar integral equation is obtained for this case.

Further details, advantages and disadvantages of these modifications of Wiener's criterion are being investigated. Y. W. Lee

6. Application of Wiener's Techniques in Transient Synthesis

In transient synthesis if $F(\lambda)$ is the transform of the driving function $f(t)$, $G(\lambda)$ the transform of the desired response function $g(t)$, then the system function $H(\lambda)$ is

$$H(\lambda) = \frac{G(\lambda)}{F(\lambda)} \quad . \tag{1}$$

For the case of $F(\lambda)$ having zeros in the lower half plane, $H(\lambda)$ is not realizable. A solution for the problem of finding the "best" $H(\lambda)$ under this condition may be obtained by considering the instantaneous difference between the actual response $f_o(t)$ and $g(t)$ and taking the integral of the square of the difference as a measure of error. Of course, this integral is assumed to be finite. Thus

$$\mathcal{E} = \int_{-\infty}^{\infty} \left[f_o(t) - g(t)\right]^2 dt \quad . \tag{2}$$

By application of the convolution integral relating $f(t)$, $f_o(t)$ and the unit-impulse response characteristic $h(t)$ of the system, it can be shown that

$$\mathcal{E} = \int_{-\infty}^{\infty} h(\tau)d\tau \int_{-\infty}^{\infty} h(\sigma)d\sigma\ \phi_{ff}(\tau - o)$$

$$-2\int_{-\infty}^{\infty} h(\tau)d\tau\ \phi_{fg}(\tau) + \phi_{gg}(0) \quad . \tag{3}$$

Here $\phi_{ff}(\tau)$ and $\phi_{gg}(\tau)$ are autocorrelation functions defined as

$$\phi_{ff}(\tau) = \int_{-\infty}^{\infty} f(t)f(t + \tau)dt \tag{4}$$

and

$$\phi_{gg}(\tau) = \int_{-\infty}^{\infty} g(t)g(t + \tau)\ dt \quad , \tag{5}$$

and $\phi_{fg}(\tau)$ is a crosscorrelation function defined by the equation

$$\phi_{fg}(\tau) = \int_{-\infty}^{\infty} f(t)g(t + \tau)dt \quad . \tag{6}$$

It is assumed that the correlation functions exist. The minimization of the integral square error results in the Wiener-Hopf equation

$$\phi_{fg}(\tau) = \int_{-\infty}^{\infty} h(\sigma)\,\phi_{ff}(\tau - \sigma)d\sigma \qquad \text{for } \tau \geq 0 \quad . \tag{7}$$

The solution of this equation gives the best $h(t)$ on the basis of minimum integral square error. The transform of $h(t)$ is $H(\lambda)$. The known solution of Eq. (7) is

$$H(\lambda) = \frac{1}{2\pi\Phi^{+}_{ff}(\lambda)} \int_{o}^{\infty} \Psi(t) e^{-j\lambda t}\, dt \qquad (8)$$

where

$$\Psi(t) = \int_{-\infty}^{\infty} \frac{\Phi_{fg}(\lambda)}{\Phi^{-}_{ff}(\lambda)} e^{j\lambda t}\, d\lambda \quad . \qquad (9)$$

The functions $\Phi_{ff}(\lambda)$ and $\Phi_{fg}(\lambda)$ are Laplace transforms of $\phi_{ff}(\tau)$ and $\phi_{fg}(\tau)$ respectively. The function $\Phi_{ff}(\lambda)$ is factored into the conjugate factors $\Phi^{+}_{ff}(\lambda)$ and $\Phi^{-}_{ff}(\lambda)$, the former containing all poles and zeros in the upper half plane and the latter all poles and zeros in the lower half plane. Illustrations are being prepared.

Y. W. Lee

7. Techniques of Optimum Filter Design

The significance of the mean-square-error criterion in communication problems has long been a subject of controversy. In a majority of cases in which this criterion has been used, its choice was made for reasons of mathematical expediency despite the fact that it lacks an extensive physical justification. One of the more outstanding applications of the rms criterion was made by N. Wiener in his theory on the design of optimum linear systems. The importance of his contribution to the philosophy of network design should not be underestimated; however, the usefulness of his approach in a practical system design may be questioned simply because of its dependence on the rms criterion. It is one of the main purposes of this study to evaluate in some measure the performance of linear filters designed according to the Wiener theory on the basis of experimental results.

The theory of optimum networks treats message and disturbance time functions which are stationary random; in particular, functions which have definite autocorrelation and power-spectrum functions. In order to facilitate the experimental procedures to be used in the interpretation of optimum-filter performance, it is desirable that the message and disturbance time functions have statistical properties which converge rapidly to their long time average values. Gaussian noise, such as the shot noise of a vacuum tube or the thermal noise of a resistor, is highly satisfactory in this respect, and is a natural choice as a disturbance time function. Messages which are usually employed in practice, such as speech or music, appear to converge too slowly statistically to be appropriate in this experiment; errors caused by short-time deviations of their statistical properties from

the long-time averages may obscure the ability of the network to recover the message from a mixture of message and disturbance. The method of handling such messages is not included in this study. On the other hand, artificial messages which have the desired characteristics may be easily generated. A particularly simple function of this type is a square wave having zero-crossings of random occurrence, such as that shown in Fig. VIII-8.

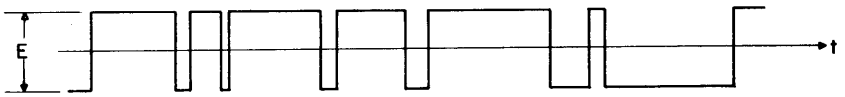

Fig. VIII-8 Square wave with zero-crossings occurring at random.

If the zero-crossings have a Poisson distribution, then the autocorrelation and power spectrum functions associated with the square wave are

$$\phi_{11}(\tau) = E^2 e^{-2k|\tau|} \tag{1}$$

$$\Phi_{11}(\omega) = \frac{2kE^2}{\pi(4k^2 + \omega^2)} \tag{2}$$

respectively, where E is the total amplitude shift in the square wave and k is the average number of zero-crossings per second. Equipment for generating such a wave has been completed.

Basically, the random-square-wave generator is a bistable multivibrator which is triggered by a sequence of pulses occurring at random. The square wave may be observed at either plate in the multivibrator, where the voltage jumps from one stable state to the other in accordance with the random triggering. A simplified form of the generator is shown in Fig. VIII-9.

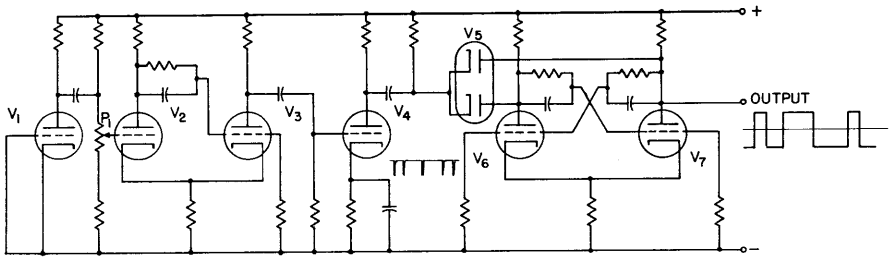

Fig. VIII-9 Simplified form of random-square-wave generator.

In this schematic V_6 and V_7 make up the two halves of the multivibrator. The random trigger pulses applied at the plates through V_5 are obtained with aid of a source of wide-band noise, which in this case is a 6D4 gas tube V_1. By means of a slicer circuit incorporating V_2 and V_3, only peaks

of the noise above a level several times the rms voltage of the noise are passed. After possible shaping and phase reversal, as in V_4, this sequence of noise peaks is used as the random trigger pulse train. Successive pulses in this train can be made independent of each other (for all practial purposes), a condition necessary for a Poisson distribution, by using a high slicing level and a large noise bandwidth. The average number of pulses per second can be varied by adjusting the slicing level, which is easily done in the circuit with aid of potentiometer P_1. In the actual generator, this average pulse rate (and consequently the average zero-crossing of the square wave) can be varied from zero to about 15,000 per sec. Representative waveforms of the output square wave are shown in the pictures of Fig. VIII-10 (a) and (b) which were taken for average zero-crossing rates of 1000 and 4000 per sec, respectively.

a. 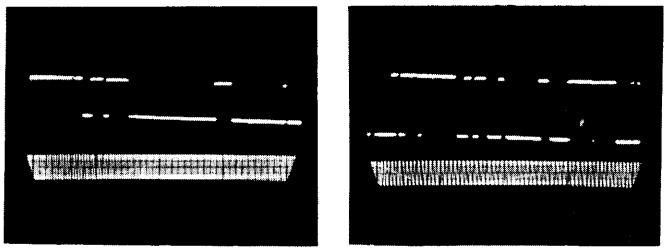 b.

Fig. VIII-10 Random square wave; timing wave is 10 kc/sec. (a) k = 1000 crossings/sec (b) k = 4000 crossings/sec.

Optimum systems, which are to be built, are now being designed for this time function as a message, and random noise as a disturbance.

Y. W. Lee, C. A. Stutt

8. Amplitude and Conditional Probability Distributions of a Quantized Time Function

In addition to the distributions discussed in the Progress Report, October 15, 1949, certain other conditional probability distributions have been studied for the voice wave instantaneous amplitude. These distributions are of the type:

$$f(x|x_1) = f\left[x(t+\tau) \middle| x_1 < x(t) < x_1 + \Delta x \right] \quad ;$$

that is, the probability density distribution that the voice wave has an amplitude x at a time $t + \tau$, having occurred in the amplitude interval $(x_1, x_1 + \Delta x)$ at time t. This type of distribution has been studied for values of τ in the range of 12 μsec to 28 msec. The shape of this

distribution is generally a single peaked curve. The shape varies from that of an impulse function centered on $x = x_1$, for short values of τ, to a form similar to that of the unconditional distribution, $f(x)$, for large values of τ. A combination of these $f(x|x_1)$ distributions with the $P(x_1|x_1)$ distributions, as mentioned in the October 15th Progress Report, provides an insight to the statistical relations between two points, spaced in time, on the voice wave.

With the completion of the above work, the study of the probability distributions concerning the voice wave instantaneous amplitude has been substantially completed. A study of certain probability distributions concerning the zero-crossing periods of the voice wave is now underway.

A major difficulty in the study of the voice wave zero-crossing periods is the effect of noise. In essence, the more efficient the apparatus is in studying the region about zero amplitude, the smaller the relative amplitude of the noise need be to cause trouble. Following the techniques of the psychacoustic experiments of Licklider, et al, a bias signal has been added to the wave so as to replace the randomly distributed noise periods with the periodic bias periods. Both supersonic (50 kcps) and low frequency (20 cps) bias signals have been used, and the effect of bias amplitude, relative to the noise amplitude, has been studied. A solution to the problem of separation of voice and noise has not yet been attained.

W. B. Davenport, Jr.

9. Storage of Pulse-Coded Information

Construction of the storage system has been completed and minor adjustments which are necessary to insure reliable operation of the equipment are being made. A technical report on the information-storage project is in preparation.

J. B. Wiesner, A. J. Lephakis

10. Felix (Sensory Replacement)

Copper electrodes have been built and tested for use in the seven-channel electrical stimulation of the forearm. At the present time we are determining how effectively a person can utilize such a system of stimulation to learn the different phonetic sounds.

J. B. Wiesner, L. Levine, O. H. Straus

11. Response of Nerve to Random Stimuli

A study has been undertaken of the frequency of firing of sensory nerves as a function of the frequency, amplitude and time distribution

of repetitive electrical stimuli. This has theoretical interest because "continuous" variables, such as temperature, force, etc., or their derivative with respect to time, constitute the input to some sensory nerves, and the nerves respond discontinuously with a pulse output whose mean frequency is some non-linear function of the input.

The problem is to characterize the time response of peripheral nerve to an input that is randomly distributed in time, and is thus closely related in method and technique to the communication studies of this laboratory. Previous physiological work has been mainly confined to short or long trains of periodic electrical stimuli. This has shown a nearly linear response rate to input frequencies below 1/t, where t = the refractory period of the nerve (corresponding to the resolution time of a counting circuit). This is unlike the physiological response of sensory nerve, which behaves in response to pressure, temperature, etc., more like a counting circuit with a fixed resolution time, an input randomly distributed in time, and a mean output rate that is a continuous non-linear function of the mean input rate.

A nerve stimulator is being constructed to provide controlled duration and amplitude square pulses which can be triggered either periodically or randomly at a controlled mean rate by means of a noise generator. These stimuli will be used to determine whether the known refractory period of peripheral nerve is sufficient to account for its physiological behavior as a transducer.

O. H. Straus

12. Speech Studies

a. A short-time correlator for speech waves

Twelve channel equipments similar to the one discussed in the last report are being constructed. Some consideration has been given to improvement of the existing delay line. This line, which was originally built to simulate a telephone line, comprises 24 low-pass filter sections (constant K section) using air-cored inductance coils. The delay of the line is very nearly constant in the frequency range of interest but the line attenuation (6 db) is considered excessive and the variation of attenuation with frequency is too great. The design and construction of an alternative delay line or other form of delay device was therefore considered.

Many of the conventional delay devices are inapplicable to this project because of the requirement for twelve values of delay. Thus, either 12 separate delay devices, or one delay device with 11 intermediate tapping points, must be used. In view of this requirement the delay line offers

advantages in that the line is readily tapped at junction points between sections and the line may be operated at such a level that the delayed speech signals at the tapping points do not require amplification before application to the multiplier circuits.

A delay line using high-Q dust-cored toroidal inductance coils was considered. By using conventional filter technique and designing the line as a low-pass filter of 50 sections, the required delay and bandwidth could be obtained. Using m-derived filter sections with $m = 1.37$ results in a uniform delay over the larger portion of the pass band (1). However a filter with $m > 1$ cannot be realized in the form of π sections, and realization in the form of T sections involves two coils per section, resulting in a cumbersome and expensive line.

A chain of band-pass-filter sections can be used as a delay line in conjunction with a modulator and detector. In the case of the short-time correlator, one input to the multiplier is required in modulated form so that the use of a band-pass delay line does not require any additional equipment. The modulated input may equally well be the delayed speech input as the direct speech input. Consequently the band-pass delay line will be fed from a balanced modulator and the delayed-modulated-speech signals from the various tapping points on the line will be fed directly to the multiplier circuits. The block diagram of Fig. VIII-11 illustrates one channel of the short-time correlator using a band-pass delay line.

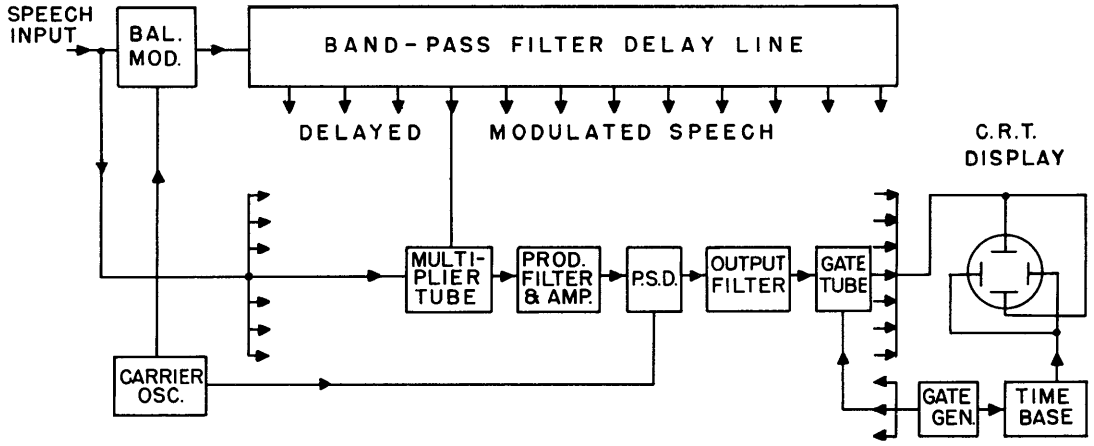

Fig. VIII-11 Block diagram of one channel of correlator using band-pass delay line.

The band-pass delay line will be made in 12 parts, each part comprising about 15 inductively-coupled tuned circuits. The coils are π wound on a 3/8 in. diam bakelite tube and are uniformly spaced except for the end coils.

In order to insure that negligible coupling exists between coils other than adjacent ones, the coil assembly is mounted concentrically in a metallic tube. The function of the tube may be explained as follows. In free space the decay of the magnetic field along the axis of a coil is approximately proportional to the cube of the distance from the coil for those distances which exceed the diameter. The metallic tube however acts as a waveguide below cut-off, and the decay of magnetic field is exponential. The mutual inductance between a number of uniformly spaced coils in various shapes and sizes of tube has been obtained experimentally. A delay of approximately 140 μsec is expected for each part of the line, giving a total delay of about 1,660 μsec.

The relative advantages of the band-pass delay line as compared with the conventional low-pass line are that variation of the attenuation with frequency can be made smaller, inexpensive air-cored coils can be used, and it occupies less space.

The relative disadvantage is that the loss per unit delay is much larger when using convenient components and necessitates the use of amplifiers at intervals along the line. The advantages are considered to outweigh heavily the disadvantages in this application.

Reference

(1) H. E. Kallman, "Equalised Delay Lines", Proc. I.R.E. 34, 646 (1946).

b. Speech synthesizer

The short-time correlator will provide a visual pattern of speech in the time domain, as contrasted with the spectrograms used at present for visual speech. Ultimately the output of the thirteen correlator channels may also be used to synthesize speech either locally or after transmission at a distant point. The details of the synthesizer have not yet been worked out, but such a scheme would perform in the time domain an analysis and synthesis similar to that produced by the vocoder in the frequency domain.

R. M. Fano, P. E. A. Cowley

c. The effect of syllabic rate on speech intelligibility

One property of the ear about which very little is known is its ability to discriminate between sounds occurring in rapid succession. A method suggested by Dr. Licklider of Harvard for study of this property is to

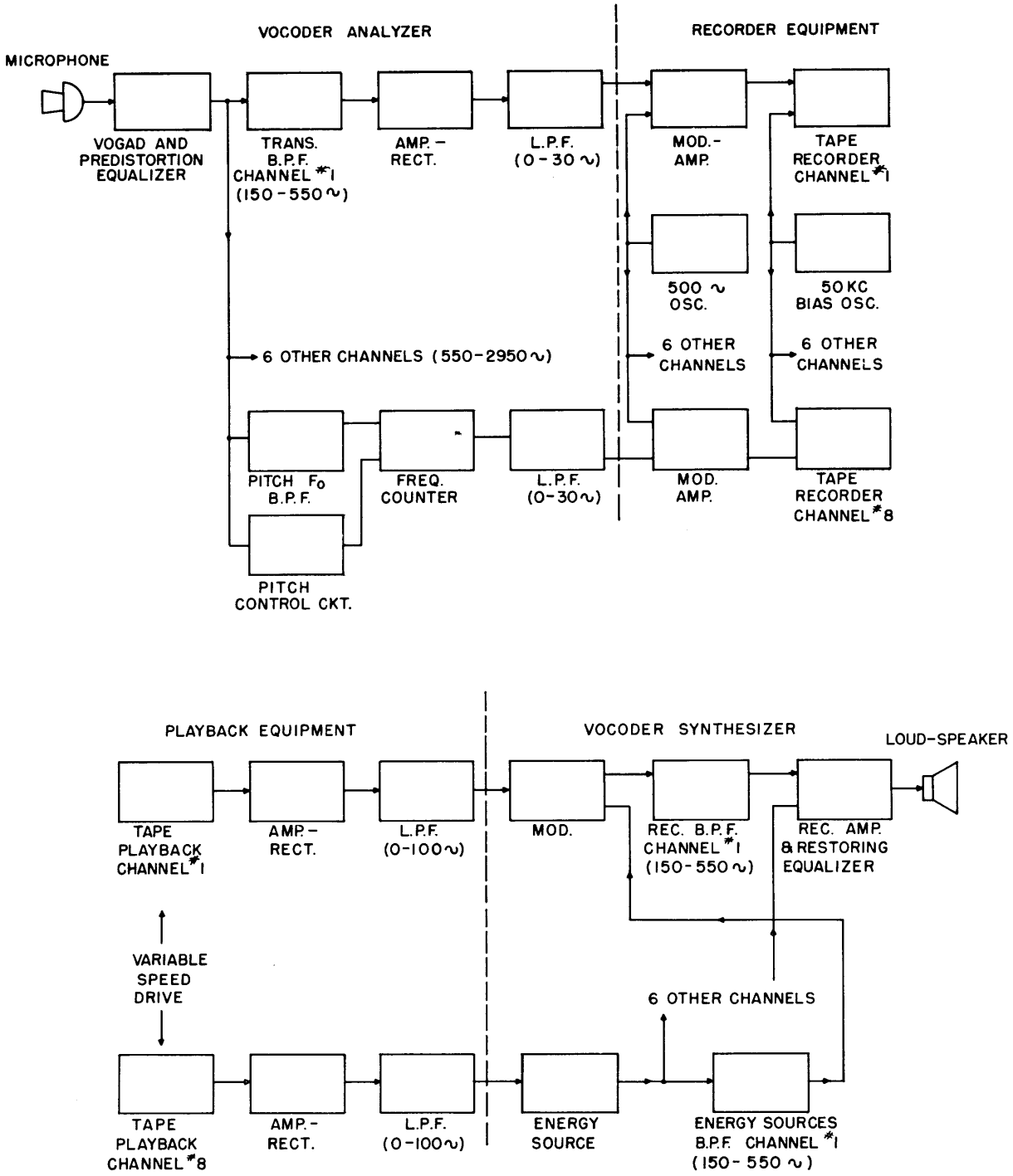

Fig. VIII-12 Block diagram of speech speed increaser.

determine the effect of the speed at which speech is spoken on its intelligibility. By using the vocoder developed by the Bell Telephone Laboratories and making certain alterations, recorded speech can be played back at any desired speed without changing its fundamental pitch. This is accomplished by recording each channel output of the vocoder analyzer simultaneously on a multi-channel magnetic tape recorder and then playing this tape into the channel inputs of the vocoder synthesizer at the desired increase in speed. Since the pitch of the voice manufactured by the synthesizer is derived from an oscillator whose fundamental frequency is dependent only on the magnitude and not on the frequency of its control channel, and since this magnitude is not changed by speeding up the tape, the pitch of the voice output remains unchanged regardless of the speed of talking.

A block diagram of the equipment is shown in Fig. VIII-12. It was deemed expedient to modulate each of the 0-30 cycle vocoder channels on a 500-cycle carrier before recording in order to eliminate any distortion of the low-frequency signal by wow in the recorder. The recorder to be used in the tests is driven by a synchronous motor and it is planned to vary the speed of playback by driving the motor from a variable-frequency source, thus giving continuously variable control of the speed.

The design of the recording equipment has been completed and preliminary tests are being made on a single channel. It is hoped that the construction of the complete equipment and its testing will be finished by the time this report is published.

R. M. Fano, J. Fairfield, Jr.

13. Pulse Coding of Picture Signals

The purpose of this work is to initiate an investigation of the redundancy problem in television. In the first part of the study, for simplification with regard to time, a facsimile (wire-photo) system, which requires 7 minutes for the transmission of one picture, is being used in place of television, which requires only one-thirtieth of a second. The facsimile system also approaches the ideal picture transmission system more closely than present-day television so that fewer errors have to be accounted for.

The first phase of the work consists of designing and building a pulse coder and decoder to be used in the transmission path between the facsimile transmitter and receiver. Provisions will be made for 2 to 256 levels and for several different sampling rates. A block diagram of the system together with corresponding waveforms is shown in Fig. VIII-13(a) and (b). A breadboard model including the first two stages of the binary counter has been built and is in working order. The complete system is now in process of construction.

The equipment will be used to determine the number of levels required to transmit a picture of a given quality. The quality of the transmission will be measured objectively by means of a reflectometer. It is also

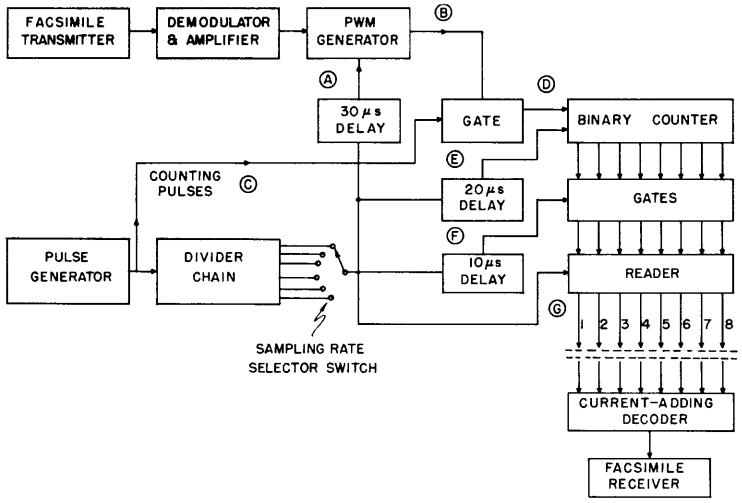

Fig. VIII-13(a)

Block diagram of coding and decoding circuit.

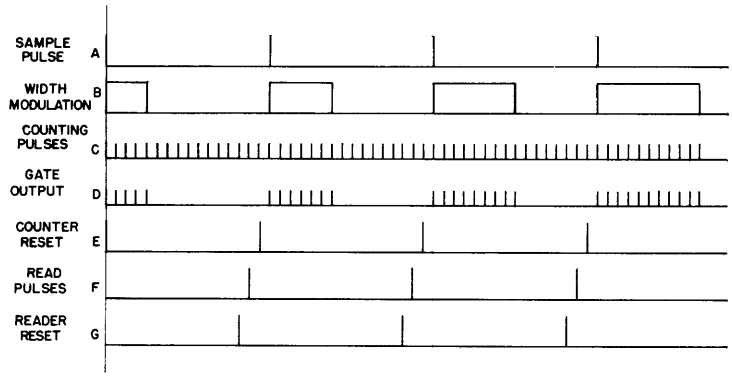

Fig. VIII-13(b)

Wave forms at specified points.

planned to use the equipment in evaluating the information content of typical pictures in order to establish bandwidth requirements for television transmission. J. B. Wiesner, H. E. Singleton, E. H. Gibbons

14. Pulse-Code Magnetic Recorder

An erasing head of high-μ iron laminations has been constructed and the Magnecord 50-kc oscillator, available in the driving unit, adjusted for the new purpose. Although the maximum current in the erasing head is about 20 percent lower than in the normal Magnecord erasing head, the erasing effect appears to be satisfactory, at least for the present purpose. (The decrease of the signal level after erasure was found to be more than 20 db.)

The coder circuits have been investigated in detail and several

alterations and additions have been made. The block diagram of the coder in its present form is shown in Fig. VIII-14. Due to the finite rise time of the phantastron circuit during the return period it was found necessary

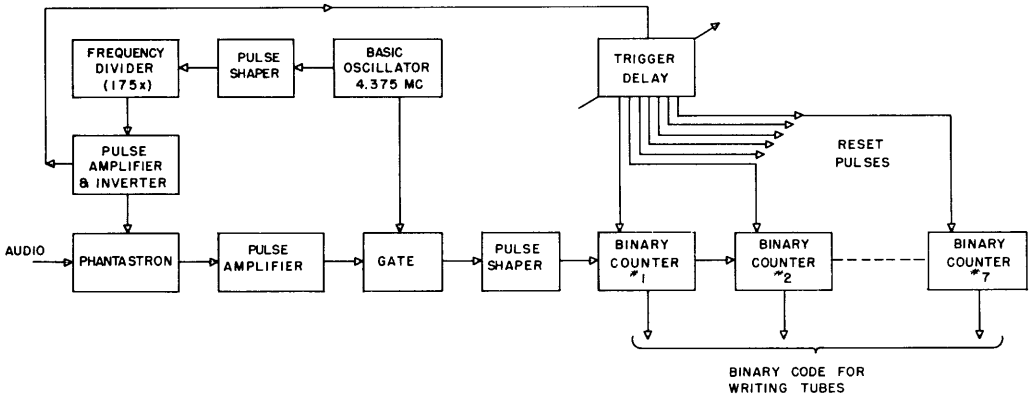

Fig. VIII-14 Block diagram of the coder.

to increase the basic oscillator frequency from 3.6 Mc to 4.375 Mc. The sampling frequency (25 kc) is derived from the basic frequency by means of a frequency divider after the sine-wave has been shaped into sharp pulses. The output of the frequency divider is then amplified and inverted to trigger the phantastron circuit every 40 μsec. The output of the phantastron is a pulse which occurs every 40 μsec and whose length is proportional to the instantaneous input voltage at the beginning of the pulse. This time-modulated pulse is then used, after amplification, to gate a continuous train of pulses coming from the basic oscillator mentioned above.

The voltage is now expressed by a train of pulses whose number is proportional to the voltage measured from some constant level. The pulses are then counted by a set of binary counter stages. At the end of the pulse train the voltages at the plates of these flip-flops express the voltage in the form of on-off potentials, i.e. in the form of a binary code. These voltages are to be fed to the suppressor grids of the writing tubes in order to allow or prevent a pulse's recording on magnetic tape.

After the recording has been performed, it is necessary to reset the counters to the zero position. This is done not before the pulse train begins to come to the counters, but rather about 2 μsec later. In this way the first few pulses are discarded and the counting really starts after this short delay. The reason for this procedure is the initial non-linearity of the phantastron circuit. We obtain in this way a constant change in d-c level, which is unimportant, but the relationship between the input voltage

and the corresponding pulse train remains linear. A similar effect could be obtained by adjusting the audio input in such a way that it would never come into the region of non-linearity. But this would restrict the number of available quantising levels since, for example, the first 15 pulses (or less) would have to be counted for each sample, but could never be used to represent a sample. In view of the circumstances the present arrangement appears to be more efficient. J. B. Wiesner, L. Dolansky

15. Twin-Track Recorder for Slow Phenomena

An apparatus is being developed to make permanent records of phenomena whose frequency spectra lie in the range of 1 to 100 cycles. This should facilitate the analysis of electroencephalographic and similar information by electronic correlation techniques. A means will be provided for speeding up the playback if necessary so that the output frequencies will fall into a range more conveniently handled by the correlator. A dual channel system is to be used, so that crosscorrelation functions can be computed for two signals from different but possibly related sources.

Due to the difficulty of recording such low-frequency signals directly on magnetic tape, some form of modulation of a carrier of more reasonable frequency must be used. An AM system has been tested and found unsatisfactory because of spurious amplitude variations on playback caused by non-uniformity of the magnetic properties of the tape.

An FM system is now being tried in which deviations as large as 40 percent of center frequency will be used. It is hoped that this will minimize the effects of tape speed variations. P. E. Green, Jr.

C. TRANSIENT PROBLEMS

Prof. E. A. Guillemin
Prof. J. C. F. Rybner (guest)
Dr. M. V. Cerrillo
W. H. Kautz
L. Weinberg

1. Transient Theories

Work on this project has been concentrated along the following lines: (1) the evaluation of certain complex prototype integrals which form the class of "transient generating functions", (2) the development of a theory of approximation for single-valued and for individual branches of multi-valued functions of a complex variable, (3) the application of the extended saddle-point method of integration to a number of examples.

Item (1) includes not only the numerical computation of these integrals

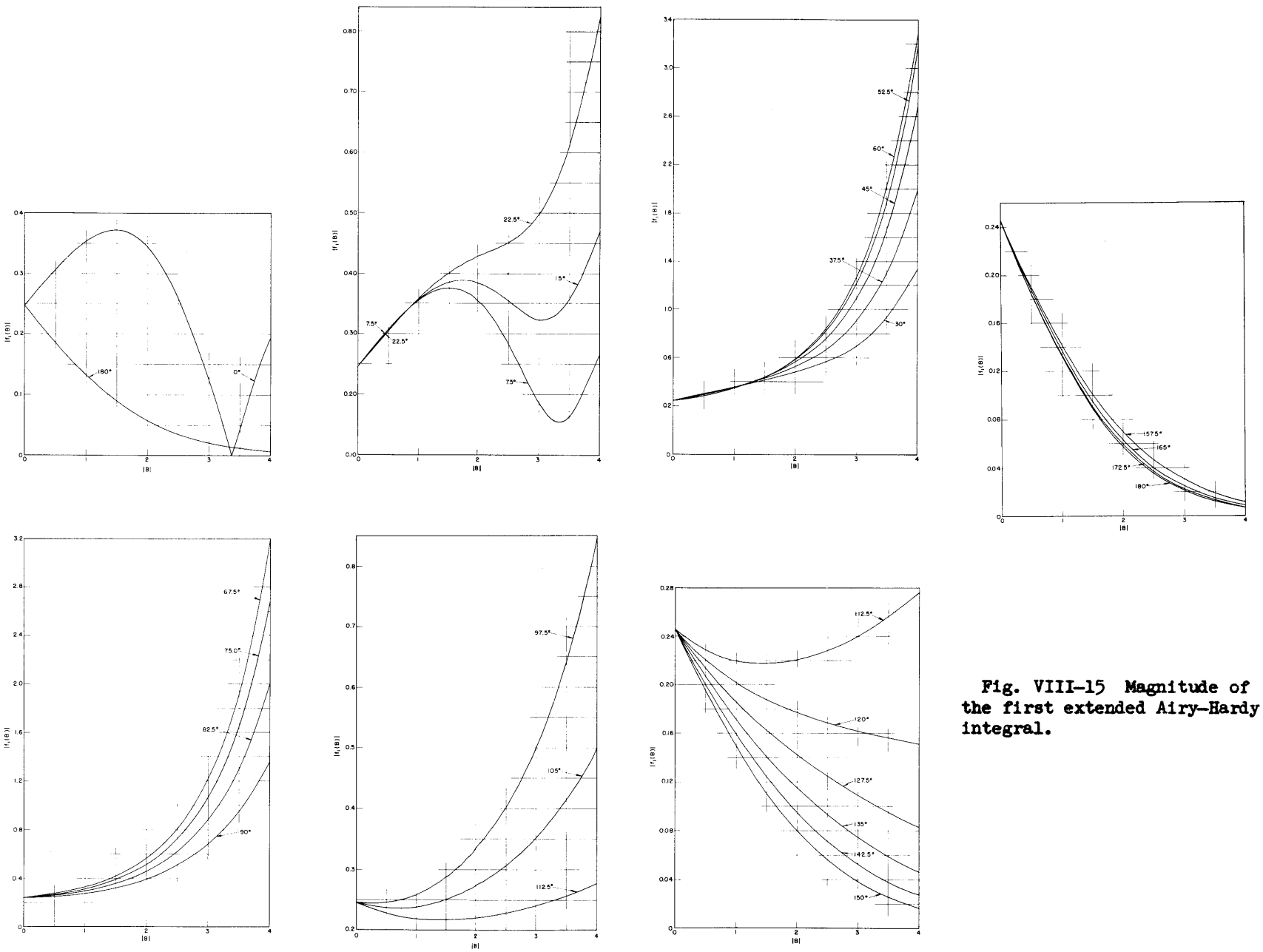

Fig. VIII-15 Magnitude of the first extended Airy-Hardy integral.

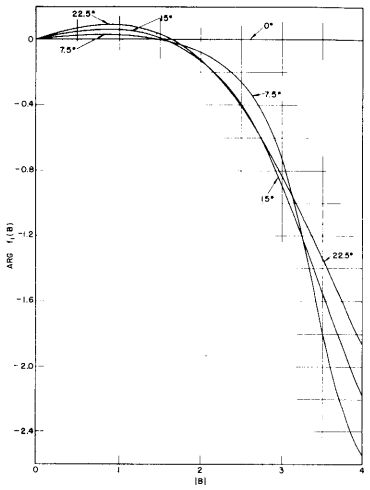

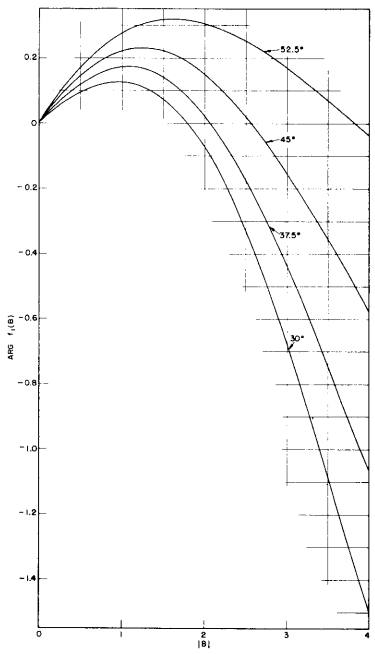

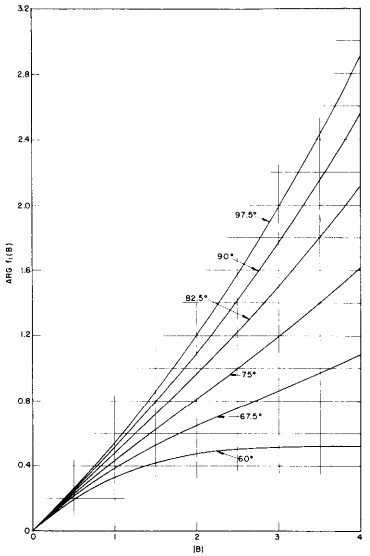

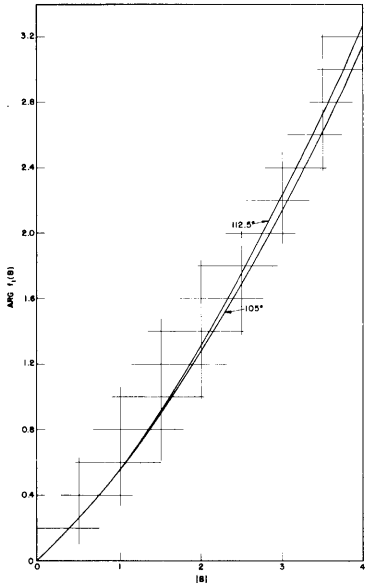

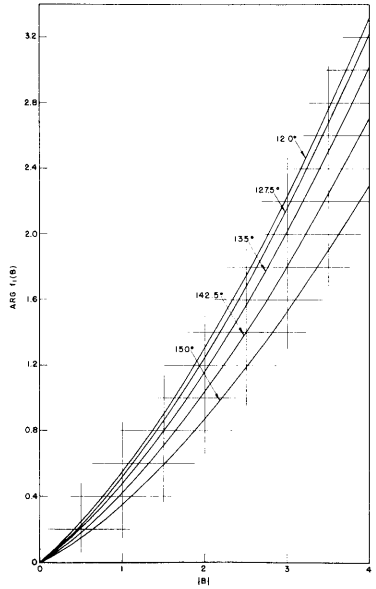

Fig. VIII-16 Phase of the first extended Airy-Hardy integral.

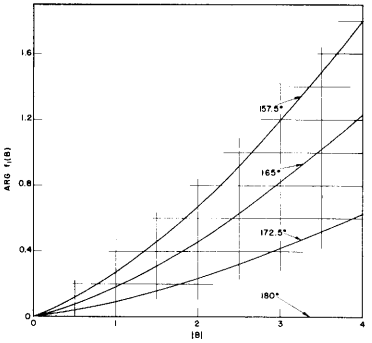

but also the development of suitable power-series and asymptotic expansions which may profitably replace the generating functions for certain values of their arguments. An attempt is also being made to prepare plots of most of these functions which include the generalized Fresnel integral, the extended Airy-Hardy integral (R.L.E. Technical Report No. 144, forthcoming), and the Lommel generating functions (R.L.E. Technical Report No. 138, forthcoming).

Approximation methods supplementary to the new theory of integration have been worked out for several types of functions likely to occur in the integrand of a complex transient integral (inverse Laplace transform). The application of continued fractions as discussed in the Progress Report, October 15, 1949, has been investigated more fully, and this sort of representation has proven to be even more useful than was anticipated at first. The primary difficulty at present is the problem of integrating through a region containing a large number of poles so as to separate the predominant resonance from the overall envelope variations and phase deviations.

Not much progress has been made along this line as yet. All these topics will be discussed fully in R.L.E. Technical Report No. 55.

As mentioned in item (3) a few simple examples of the use of the saddle-point method are being worked out. In certain cases the results are obtained quickly and neatly but in other more practical examples, some refinement of the procedure will be necessary before it can be universally applied to the large class of problems to which it is applicable.

Plots in Figs. VIII-15 and VIII-16 show the magnitude and phase of the first extended Airy-Hardy integral, mentioned in a previous Progress Report:

$$f_1(B) = \frac{1}{2\pi i} \int_{\gamma_1(z)} e^{Bz+z^3}\, dz \quad .$$

Here $\gamma_1(z)$ is any contour from $\infty \cdot e^{-i\pi/3}$ to $\infty \cdot e^{i\pi/3}$ through the finite part of the z-plane.

In the theory of synthesis of electrical networks and other similar systems it is of basic importance to develop mathematical relations connecting entities in the time and frequency domains. These relationships are of primary importance in the theory of FM transients and in pure mathematical analysis. These relations between the time and frequency domains are very hard to discover if one considers the integral character of the transformation involved. Evaluations of the transformation as $s \to \infty$, $s = 0$, $t = 0$ and $t \to \infty$ were well known long ago, but nothing else can be said

about such relationships in general.

The methods of integration which are being investigated by this group show some approximate methods for visualizing certain pertinent time-frequency relations. A new discovery in this connection is reported here. The new property reads:

Let f(t) be Laplace transformable, having F(s) as its Laplace transform. If f(t) has the form $f(t) = f_1(t)e^{\phi(t)}$, $f_1(t)$ and $\phi(t)$ being rational or algebraic functions, and if F(s) has the form $f(t) = F_1(s)e^{\Psi(s)}$, $F_1(s)$ and $\Psi(s)$ being rational or algebraic functions, $\mathcal{L} f_1(t) \neq F_1(s)$.

If one sets

$$s = \phi'(t) = \frac{d\phi(t)}{dt}$$

$$t = \Psi'(s) = \frac{d\Psi(s)}{ds}$$

Then $-\Psi'(s) = \phi'^{(-1)}(s)$ in which $\phi'^{(-1)}(s)$ means the solution for t of $s = \phi'(t)$.

Under the above assumptions, one may also derive the equivalent property

$$F(s) = \int_0^\infty f_1(t)e^{-st+\phi(t)}\,dt$$

$$f(t) = \frac{1}{2\pi i}\int_{c-i\infty}^{c+i\infty} F_1(s)e^{st+\Psi(s)}\,ds$$

Let $a(t,s) = -st - \phi(t)$ $\quad a'(t,s) = 0 = -s + \phi'(t)$ $\quad \therefore s = \phi'(t)$

$W(s,t) = st + \Psi(s)$ $\quad W'(s,t) = 0 = t + \Psi'(s)$ $\quad \therefore t = -\Psi'(s)$

which means that the saddle points in the s plane are the images of the saddle points in the (complex) t plane, since $\phi'(t)$ and $-\Psi(s)$ are inverse functions.

The proof of this property was made by applying heuristic reasoning to the above integrals. Since these methods yield approximate solutions, the generality of the above property is limited by the conditions stated in the theorem. Nevertheless, the theorem may also hold when f(t) and F(s) show exponential behavior in certain parts of the t and s planes, respectively. A list of transform pairs for which the above property holds is given in Tables I to XIII.

Table I

EXPONENTIALS IN THE TIME DOMAIN

$\mathcal{L}$

1. $e^{-\frac{a^2}{4t}} = \sqrt{\frac{\pi}{s}}\, e^{-a\sqrt{s}}$

2. $\frac{a^{2\nu+2}}{(2t)^{\nu+1}} e^{-\frac{a^2}{4t}} = a^{\nu+2}\, s^{\frac{\nu}{2}}\, K_\nu(a\sqrt{s})$

3. $\frac{e^{-2\sqrt{t}}}{\sqrt{\pi t}} = \frac{1}{\sqrt{s}}\, e^{\frac{1}{s}}\, \mathrm{erfc}(\frac{1}{s})$

4. $\frac{1}{\sqrt{\pi t}} \frac{d^n}{dx^n} e^{-\frac{x^2}{4t}} = (-1)^n\, s^{\frac{n-1}{2}}\, e^{-x\sqrt{s}}$

5. $e^{-t^2} = \frac{\sqrt{\pi}}{2}\, e^{\frac{s^2}{4}}\, \mathrm{erfc}(\frac{s}{2})$

6. $t^{\nu-1} e^{-t^2} = \frac{\Gamma(\nu)}{2^{\frac{\nu}{2}}}\, e^{\frac{s^2}{8}}\, D_{-\nu}(\frac{s}{\sqrt{2}})$

7. $t^{\frac{\nu}{2}} e^{-\sqrt{t}} = \Gamma(\nu+1)\, s^{-\frac{2+\nu}{2}}\, e^{\frac{1}{8s}}\, D_{-(\nu+1)}(\sqrt{\frac{2}{s}})$

Key: $K_\nu(x)$ behaves as e^{-x}

$\mathrm{erfc}(\frac{1}{s})$ does not have exponential behavior

$D_{-\nu}(x)$ behaves as $e^{+\frac{x^2}{4}}$

Table II

CIRCULAR FUNCTIONS IN THE TIME DOMAIN

$\mathcal{L}$

1. $\frac{\cos\sqrt{t}}{\sqrt{t}} = \sqrt{\frac{\pi}{s}}\, e^{-\frac{1}{4s}}$

2. $\sinh b\sqrt{t} = \frac{b}{2}\frac{1}{s}\sqrt{\frac{\pi}{s}}\, e^{-\frac{b^2}{4s}}$

3. $\sqrt{t}\,\cosh b\sqrt{t} = \frac{b}{2}\frac{1}{s}\sqrt{\frac{\pi}{s}}\left(1 - \frac{b^2}{4s}\right) e^{-\frac{b^2}{4s}}$

4. $e^{-at}\frac{\cos\sqrt{t}}{\sqrt{t}} = \sqrt{\pi}\,\frac{e^{-\frac{1}{4(s+a)}}}{\sqrt{s+a}}$

5. $t^{-\frac{3}{4}} \sin\sqrt{8t} = 2^{\frac{1}{4}}\pi\,\frac{1}{\sqrt{s}}\, e^{-\frac{1}{s}}\, I_{\frac{1}{4}}(\frac{1}{s})$

6. $t^{-\frac{3}{4}} \cos\sqrt{8t} = 2^{\frac{1}{4}}\pi\,\frac{1}{\sqrt{s}}\, e^{-\frac{1}{s}}\, I_{\frac{1}{4}}(\frac{1}{s})$

Key: $\left.\begin{matrix}\cos x \\ \sin x\end{matrix}\right\}$ behave as e^{ix}

$I_{\frac{1}{4}}(x)$ behaves as e^{-x}

$I_{-\frac{1}{4}}(x)$ behaves as e^{+x}

Table III

HYPERBOLIC FUNCTIONS IN THE TIME DOMAIN

$\mathcal{L}$

1. $\sinh\sqrt{t} = \frac{1}{2s}\sqrt{\frac{\pi}{s}}\, e^{\frac{1}{4s}}$

2. $\frac{\cosh\sqrt{t}}{\sqrt{t}} = \sqrt{\frac{\pi}{s}}\, e^{\frac{1}{4s}}$

3. $e^{-at}\sinh(2b\sqrt{t}) = \frac{\sqrt{\pi}\, b}{(s+a)^{\frac{3}{2}}}\, e^{\frac{b^2}{s+a}}$

4. $e^{-at}\frac{\cosh(2b\sqrt{t})}{\sqrt{t}} = \sqrt{\frac{\pi}{s+a}}\, e^{\frac{b^2}{s+a}}$

5. $\sqrt{t}\cosh(b\sqrt{t}) = \frac{1}{2s}\sqrt{\frac{\pi}{s}}\, e^{\frac{b^2}{4s}}\left(1 + \frac{b^2}{2s}\right)$

6. $t^{-\frac{3}{4}}\sinh(\sqrt{8t}) = 2^{\frac{1}{4}}\frac{\pi}{\sqrt{s}}\, e^{\frac{1}{s}}\, I_{\frac{1}{4}}(\frac{1}{s})$

7. $t^{-\frac{3}{4}}\cosh(\sqrt{8t}) = 2^{\frac{1}{4}}\frac{\pi}{\sqrt{s}}\, e^{\frac{1}{s}}\, I_{-\frac{1}{4}}(\frac{1}{s})$

8. $\sinh(\sqrt{t}) + \sin(\sqrt{t}) = \frac{1}{s}\sqrt{\frac{\pi}{s}}\cosh(\frac{1}{4s})$

9. $\sinh(\sqrt{t}) - \sin(\sqrt{t}) = \frac{1}{s}\sqrt{\frac{\pi}{s}}\sinh(\frac{1}{4s})$

10. $t^{-\frac{1}{2}}\left[\cosh(\sqrt{t}) + \cos(\sqrt{t})\right] = 2\sqrt{\frac{\pi}{s}}\cosh(\frac{1}{4s})$

11. $t^{-\frac{1}{2}}\left[\cosh(\sqrt{t}) - \cos(\sqrt{t})\right] = 2\sqrt{\frac{\pi}{s}}\sinh(\frac{1}{4s})$

12. $\sqrt{t}\left[\cosh(\sqrt{t}) + \cos(\sqrt{t})\right] = \frac{1}{s}\sqrt{\frac{\pi}{s}}\left[\cosh(\frac{1}{4s}) + \frac{1}{2s}\sinh(\frac{1}{4s})\right.$

13. $\sqrt{t}\left[\cosh(\sqrt{t}) - \cos(\sqrt{t})\right] = \frac{1}{s}\sqrt{\frac{\pi}{s}}\left[\sinh(\frac{1}{4s}) + \frac{1}{2s}\cosh(\frac{1}{4s})\right.$

14. $2^{\frac{3}{4}}t^{-\frac{3}{4}}\left[\sinh(\sqrt{8t}) + \sin(\sqrt{8t})\right] = \frac{\pi}{\sqrt{s}}\, I_{\frac{1}{4}}(\frac{1}{s})\cosh(\frac{1}{s})$

15. $2^{\frac{3}{4}}t^{-\frac{3}{4}}\left[\sinh(\sqrt{8t}) - \sin(\sqrt{8t})\right] = \frac{\pi}{\sqrt{s}}\, I_{\frac{1}{4}}(\frac{1}{s})\sinh(\frac{1}{s})$

16. $2^{\frac{3}{4}}t^{-\frac{3}{4}}\left[\cosh(\sqrt{8t}) + \cos(\sqrt{8t})\right] = \frac{\pi}{\sqrt{s}}\, I_{-\frac{1}{4}}(\frac{1}{s})\cosh(\frac{1}{s})$

17. $2^{\frac{3}{4}}t^{-\frac{3}{4}}\left[\cosh(\sqrt{8t}) - \cos(\sqrt{8t})\right] = \frac{\pi}{\sqrt{s}}\, I_{-\frac{1}{4}}(\frac{1}{s})\sinh(\frac{1}{s})$

Key: In 8, 9, 10, 11, 12, 13, 14, 15, 16 and 17 the first member behaves as e^{x}, $I_{\frac{1}{4}}(x)$ and $I_{-\frac{1}{4}}(x)$ as e^{-x}.

Table IV

ERROR INTEGRAL FUNCTIONS IN THE TIME DOMAIN

$\mathcal{L}$

1. $2\sqrt{\frac{t}{\pi}}\, e^{-\frac{a^2}{4t}} - a\,\mathrm{erfc}\left(\frac{a}{2\sqrt{t}}\right) = \frac{1}{s\sqrt{s}}\, e^{-a\sqrt{s}}$

2. $a\sqrt{\frac{t}{\pi}}\, e^{-\frac{a^2}{4t}} + \left(t + \frac{a^2}{2}\right)\mathrm{erf}\frac{a}{2\sqrt{t}} - \frac{a^2}{2} = \frac{1 - e^{-a\sqrt{s}}}{s^2}$

Key: erf(x) and erfc(x) do not have exponential behavior.

Table V

BESSEL FUNCTIONS OF THE FIRST KIND IN THE TIME DOMAIN

$\mathcal{L}$

1. $$t^{\frac{\nu}{2}} J_\nu(2\sqrt{at}) = \frac{a^{\frac{\nu}{2}}}{s^{\nu+1}} e^{-\frac{a}{s}}$$

2. $$J_0(2\sqrt{at}) = \frac{1}{s} e^{-\frac{a}{s}}$$

3. $$J_{n+\frac{1}{2}}\left(\frac{t^2}{2}\right) = \frac{\Gamma(n+1)}{\sqrt{s}} D_{-(n+1)}\left(se^{\frac{\pi i}{4}}\right) D_{-(n+1)}\left(se^{-\frac{\pi i}{4}}\right)$$

4. $$J_\nu(2\sqrt{t}) = \frac{1}{2s}\sqrt{\frac{1}{s}}\, e^{-\frac{1}{2s}} \left[I_{\frac{\nu-1}{2}}\left(\frac{1}{2s}\right) - I_{\frac{\nu+1}{2}}\left(\frac{1}{2s}\right)\right]$$

5. $$t^{n+\frac{\alpha}{2}} J_n(2\sqrt{t}) = \frac{n!\, e^{-\frac{1}{s}}}{s^{n+\alpha+1}} L_n^\alpha\left(\frac{1}{s}\right)$$

6. $$\frac{J_0(a\sqrt{t})}{\sqrt{t}} = \sqrt{\frac{\pi}{s}}\, e^{-\frac{a^2}{8s}} I_0\frac{a^2}{8s}$$

7. $$t^n J_0(2\sqrt{t}) = \frac{e^{-\frac{1}{s}}}{s^{n+1}} L_n\left(\frac{1}{s}\right)$$

8. $$\sum_{n=0}^{\infty} J_{2\nu+2n+1}(4\sqrt{t}) = \frac{1}{s}\sqrt{\frac{\pi}{s}}\, e^{-\frac{2}{s}} J_\nu\left(\frac{2}{s}\right)$$

9. $$J_0^2(2a\sqrt{t}) = \frac{1}{s} e^{-\frac{2a^2}{s}} I_0\left(\frac{2a^2}{s}\right)$$

10. $$J_0(2a\sqrt{t}) J_0(2b\sqrt{t}) = \frac{1}{s} e^{-\frac{a^2+b^2}{s}} I_0\left(\frac{2ab}{s}\right)$$

11. $$J_0(2a\sqrt{t}) I_0(2b\sqrt{t}) = \frac{1}{s} e^{-\frac{a^2-b^2}{s}} J_0\left(\frac{2ab}{s}\right)$$

12. $$\frac{J_0^2(2\sqrt{t})}{t} = \frac{1}{s} e^{-\frac{2}{s}} \left[I_0\left(\frac{2}{s}\right) + 2\sum_{s=1}^{\infty} I_{0+s}\left(\frac{1}{s}\right)\right]$$

13. $$t^{\frac{\nu}{2}} \left[J_\nu(2\sqrt{t}) - I_\nu(2\sqrt{t})\right] = \frac{2}{s^{\nu+1}} \sinh\left(\frac{1}{s}\right)$$

14. $$t^{\frac{\nu}{2}} \left[J_\nu(2\sqrt{t}) + I_\nu(2\sqrt{t})\right] = \frac{2}{s^{\nu+1}} \cosh\left(\frac{1}{s}\right)$$

15. $$\frac{J_{2n}(2a\sqrt{t})}{\sqrt{t}} = \sqrt{\frac{\pi}{s}}\, e^{-\frac{a^2}{2s}} I_n\left(\frac{a^2}{2s}\right)$$

16. $$J_0\left(a\sqrt{t^2 - k^2}\right) = \frac{e^{-k\sqrt{s^2+a^2}}}{\sqrt{s^2 + a^2}}$$

17. $$J_0\left(a\sqrt{t^2 + 2kt}\right) = \frac{e^{-k\left(\sqrt{s^2+a^2} - s\right)}}{\sqrt{s^2 + a^2}}$$

18. $$\frac{t-k}{t+k}^{\frac{1}{2}} J_\nu\left(a\sqrt{t^2 - k^2}\right) = \frac{a^\nu e}{\sqrt{s^2 + a^2}\left(\sqrt{s^2 + a^2} + s\right)^\nu}$$

19. $$I_0(2\sqrt{t}) I_0(2a\sqrt{t}) + J_0(2\sqrt{t}) J_0(2a\sqrt{t}) = \frac{2}{s} I_0\left(\frac{2a}{s}\right) \cosh\left(\frac{a^2+1}{s}\right)$$

20. $$I_0(2\sqrt{t}) I_0(2a\sqrt{t}) - J_2(2\sqrt{t}) J_0(2a\sqrt{t}) = \frac{2}{s} J_0\left(\frac{2a}{s}\right) \sinh\left(\frac{a^2+1}{s}\right)$$

Key: $J_\nu(\alpha)$ behaves as $e^{i\alpha}$, $I_\nu(\alpha)$ behaves as e^{α} } in the time domain

$I_\nu(\beta)$ behaves as $e^{-\beta}$, $J_\nu(\beta)$ behaves as $e^{-i\beta}$ } in the frequency domain

Table VI

BESSEL FUNCTIONS OF THE SECOND KIND (Y_ν) IN THE TIME DOMAIN

1. $$\mathcal{L}\,\frac{Y_0(a\sqrt{t})}{\sqrt{t}} = \frac{-1}{\sqrt{\pi s}}\, e^{-\frac{a^2}{8s}} K_0\left(\frac{a^2}{8s}\right)$$

Key: $Y_0(a\sqrt{t})$ behaves as $e^{+ia\sqrt{t}}$ $\quad$ $K_0\left(\frac{a^2}{8s}\right)$ behaves as $e^{-\frac{a^2}{8s}}$

Table VII

BESSEL FUNCTIONS OF THE THIRD KIND $H_\nu^{(1)}$ or $H_\nu^{(2)}$ IN THE TIME DOMAIN

$\mathcal{L}$

1. $$\frac{H_0^{(1)}(a\sqrt{t})}{\sqrt{t}} = \sqrt{\frac{\pi}{s}}\, e^{-\frac{a^2}{8s}} \left[I_0\left(\frac{a^2}{8s}\right) - \frac{i}{\pi} K_0\left(\frac{a^2}{8s}\right)\right]$$

2. $$\frac{H_0^{(2)}(a\sqrt{t})}{\sqrt{t}} = \sqrt{\frac{\pi}{s}}\, e^{-\frac{a^2}{8s}} \left[I_0\left(\frac{a^2}{8s}\right) + \frac{i}{\pi} K_0\left(\frac{a^2}{8s}\right)\right]$$

Key: $H_0^{(1)}(a\sqrt{t})$ behaves as $e^{ia\sqrt{t}}$ $\quad$ $I_0\left(\frac{a^2}{8s}\right)$ behaves as $e^{-\frac{a^2}{8s}}$

Table VIII

BESSEL FUNCTION OF FIRST KIND AND IMAGINARY ARGUMENT (I_ν) IN THE TIME DOMAIN

$$\mathcal{L}\left\{\begin{array}{ll}
1. & t^{\frac{\nu}{2}} I_\nu(2\sqrt{t}) = \frac{1}{s^{\nu+1}} e^{\frac{1}{s}} \\
2. & I_0(2\sqrt{t}) = \frac{1}{s} e^{\frac{1}{s}} \\
3. & I_0\left(k\sqrt{t^2 - k^2}\right) = \frac{e^{-k\sqrt{s^2-a^2}}}{\sqrt{s^2 - a^2}} \\
4. & e^{-at} I_0\left(\lambda\sqrt{t^2 - k^2}\right) = \frac{e^{-k\sqrt{(s+2a)(s+2b)}}}{\sqrt{(s + 2a)(s + 2b)}} \qquad \begin{array}{l} a = a + b \\ \lambda = a - b \end{array} \\
5. & e^{-\alpha(t+\gamma)} I_0\left(\beta\sqrt{t^2 + 2\gamma t}\right) = \frac{e^{\gamma\left(\gamma - \sqrt{(s+2a)(s+2b)}\right)}}{(s + 2a)(s + 2b)} \\
6. & I_\nu(2\sqrt{t}) = \frac{1}{2}\frac{1}{s} e^{\frac{1}{2s}}\left[I_{\frac{\nu-1}{2}}\left(\frac{1}{2s}\right) - I_{\frac{\nu+1}{2}}\left(\frac{1}{2s}\right)\right] \\
7. & t^{-\frac{1}{2}} I_{2\nu}(8\sqrt{t}) = \sqrt{\frac{\pi}{s}} e^{\frac{1}{s}} I_\nu\left(\frac{1}{s}\right) \\
8. & \sum_{n=0}^{\infty} I_{2n+2\nu+1}(4\sqrt{t}) = \frac{1}{s}\sqrt{\frac{\pi}{s}} e^{\frac{2}{s}} I_\nu\left(\frac{2}{s}\right) \\
9. & I_\nu^2(2\sqrt{t}) = \frac{1}{s} e^{\frac{2}{s}} I_\nu\left(\frac{2}{s}\right) \\
10. & \frac{I^2(2\sqrt{t})}{t} = \frac{1}{s} e^{\frac{2}{s}}\left[I_\nu\left(\frac{2}{s}\right) + 2\sum_{r=1}^{\infty} I_{\nu+r}\left(\frac{2}{s}\right)\right] \\
11. & t^{-\frac{1}{2}}\left[I_{2\nu}(\sqrt{8t}) + J_{2\nu}(\sqrt{8t})\right] = 2\sqrt{\frac{\pi}{s}} I_\nu\left(\frac{1}{s}\right)\cosh\left(\frac{1}{s}\right) \\
12. & t^{-\frac{1}{2}}\left[I_{2\nu}(\sqrt{8t}) - J_{2\nu}(\sqrt{8t})\right] = 2\sqrt{\frac{\pi}{s}} I_\nu\left(\frac{1}{s}\right)\sinh\left(\frac{1}{s}\right) \\
13. & I_\nu^2(2\sqrt{t}) + J^2(2\sqrt{t}) = \frac{2}{s} I_\nu\left(\frac{2}{s}\right)\cosh\left(\frac{2}{s}\right) \\
14. & I_\nu^2(2\sqrt{t}) - J^2(2\sqrt{t}) = \frac{2}{s} I_\nu\left(\frac{2}{s}\right)\sinh\left(\frac{2}{s}\right) \\
15. & t^{-1}\left[I_\nu^2(2\sqrt{t}) + J^2(2\sqrt{t})\right] = \frac{2}{\nu}\left[I_\nu\left(\frac{2}{s}\right) + 2\sum_{r=1}^{\infty} I_{\nu+r}\left(\frac{2}{s}\right)\right]\sinh\left(\frac{1}{s}\right) \\
16. & t^{-1}\left[I_\nu^2(2\sqrt{t}) - J_\nu^2(2\sqrt{t})\right] = \frac{2}{\nu}\left[I_\nu\left(\frac{2}{s}\right) + 2\sum_{r=1}^{\infty} I_{\nu+r}\left(\frac{2}{s}\right)\right]\sinh\left(\frac{1}{s}\right) \\
17. & I_\nu(2a\sqrt{t}) I_\nu(2b\sqrt{t}) = \frac{e^{\frac{a^2+b^2}{s}}}{s} I_\nu\left(\frac{2ab}{s}\right) \\
18. & I_\nu(2a\sqrt{t}) J_\nu(2b\sqrt{t}) = \frac{e^{\frac{a^2-b^2}{s}}}{s} J_\nu\left(\frac{2ab}{s}\right) \\
19. & I_0(2\sqrt{t}) I_\nu(2a\sqrt{t}) + J_\nu(2\sqrt{t}) J_\nu(2a\sqrt{t}) = \frac{2}{s} I_\nu\left(\frac{2a}{s}\right)\cosh\left(\frac{a^2 + 1}{s}\right) \\
20. & I_0(2\sqrt{t}) I_\nu(2a\sqrt{t}) - J_\nu(2\sqrt{t}) J(2a\sqrt{t}) = \frac{2}{s} I_\nu\left(\frac{2a}{s}\right)\sinh\left(\frac{a^2 + 1}{s}\right) \\
21. & e^{-t^2} I_\nu(t^2) = \frac{1}{\sqrt{8\pi}} e^{\frac{s^2}{16}} K_\nu\left(\frac{s^2}{16}\right)
\end{array}\right.$$

Table IX

BESSEL FUNCTIONS (K_ν) IN THE TIME DOMAIN

$$\mathcal{L}\left\{\begin{array}{ll}
1. & K_1(a\sqrt{t}) = \frac{a}{2s}\sqrt{\frac{\pi}{s}} e^{\frac{a^2}{8s}}\left[K_1\left(\frac{a^2}{8s}\right) - K_0\left(\frac{a^2}{8s}\right)\right] \\
2. & t^{-\frac{1}{2}} K(a\sqrt{t}) = \sqrt{\frac{\pi}{s}} \frac{e^{\frac{a^2}{8s}}}{2\cos\left(\frac{\nu\pi}{2}\right)} K_\nu\left(\frac{a^2}{8s}\right) \\
3. & t^{-\frac{1}{2}}\left[K_0(a\sqrt{t}) + \frac{\pi}{2} Y_0(a\sqrt{t})\right] = \sqrt{\frac{\pi}{s}}\sinh\left(\frac{a^2}{8s}\right) K_0\left(\frac{a^2}{8s}\right) \\
4. & t^{-\frac{1}{2}}\left[K_0(a\sqrt{t}) - \frac{\pi}{2} Y_0(a\sqrt{t})\right] = \sqrt{\frac{\pi}{s}}\cosh\left(\frac{a^2}{8s}\right) K_0\left(\frac{a^2}{8s}\right) \\
5. & \frac{1}{\sqrt{4\pi t}} e^{-\frac{a^2}{8t}} K_\nu\left(\frac{a^2}{8t}\right) = \frac{1}{\sqrt{s}} K_2(a\sqrt{s}) \\
6. & \sqrt{\frac{2}{\pi t}} e^{-\frac{1}{t}} K_0\left(\frac{1}{t}\right) = \sqrt{\frac{8}{s}} K_{2\nu}(\sqrt{8s})
\end{array}\right.$$

Key: In 1, 2, 3 and 4, $K_\nu(x)$ behaves as e^x
In 5 and 6, $K_\nu(x)$ behaves as e^{-x}

Table X

BESSEL FUNCTIONS OF GIOLIANI TYPE ($J_{m,n}$) IN THE TIME DOMAIN

$$\mathcal{L}\left\{\begin{array}{ll}
1. & t^{-\frac{m+n}{3}} J_{m,n}\left(3t^{\frac{1}{3}}\right) = (-1)s^{\frac{m+n-2}{2}} J_{m-n}\left(-\frac{s}{\sqrt{s}}\right) \\
2. & t^{\frac{2m-n}{3}} J_{m,n}\left(3t^{\frac{1}{3}}\right) = s^{\frac{n}{2}-m-1} J_{n}\left(-\frac{2}{\sqrt{s}}\right) \\
3. & t^{\frac{2n-m}{3}} J_{m,n}\left(3t^{\frac{1}{3}}\right) = s^{\frac{m}{2}-n-1} J_{m}\left(-\frac{2}{\sqrt{s}}\right) \\
4. & -\frac{n+m}{3} t^{-1-\frac{m+n}{3}} J_{m,n}\left(3t^{\frac{1}{3}}\right) + t^{-\frac{m+n+2}{3}} J'_{m,n}\left(3t^{\frac{1}{3}}\right) = (-1)^n s^{\frac{m+n}{2}} J_{n-m}\left(-\frac{2}{\sqrt{s}}\right) \\
5. & (t-a)^{\frac{2m-n}{3}} J_{m,n}\left[3(t-a)^{\frac{1}{3}}\right] = s^{\frac{n}{2}-m-1} e^{-as} J_{n}\left(-\frac{2}{\sqrt{s}}\right) \\
6. & J_{2m,n}\left(3t^{\frac{2}{3}}\right) = e^{-\frac{2}{s^2}} I_{n}\left(\frac{2}{s^2}\right)
\end{array}\right.$$

Key: $J_{m,n}$ behaves as $e^{(-1)^{\frac{1}{3}}x}$

Table XI

WHITTAKER FUNCTIONS ($W_{\mu,\nu}$) IN THE TIME DOMAIN

$$1.\quad \mathcal{L}\ \frac{a^{2\mu}}{t^{\mu}} e^{-\frac{a^2}{8t}} W_{\mu,\nu}\left(\frac{a^2}{4t}\right) = \frac{a^{2\mu+1}}{s^{\mu+\frac{1}{2}}} K_{2\nu}(a\sqrt{s})$$

Key: $W_{\mu,\nu}(x)$ behaves as $e^{-\frac{x}{2}}$

Table XII

WEBER FUNCTIONS (D_ν) IN THE TIME DOMAIN

$$\mathcal{L}\left\{\begin{array}{ll}
1. & D_n(t) = (-1)^n 2\pi^{\frac{n+1}{2}} \frac{e^{-s^2}}{s} \frac{d^n}{ds^n} e^{2s^2} \\
2. & (2t)^{-\frac{\nu}{2}} e^{-\frac{a^2}{8t}} D_{\nu-1}\left(\frac{a}{\sqrt{2t}}\right) = \sqrt{\frac{\pi}{2}} s^{\frac{\nu-2}{2}} e^{-a\sqrt{s}} \\
3. & e^{-\frac{t^2}{4}} \sum_{r=0}^{n} (-1)^{n-r} \frac{n!}{r![(n-r)!]^2} t^{n-r} D_{n-r}(t) = s^n e^{\frac{s^2}{4}} D_{-n-1}(s)
\end{array}\right.$$

Key: D_n behaves as $e^{-\frac{x^2}{4}}$ $\qquad$ $D_{-n-1}(x)$ behaves as $e^{+\frac{x^2}{4}}$

Table XIII

THE HERMITE POLYNOMIALS (He_n) IN THE TIME DOMAIN

$$1.\quad \mathcal{L}\ \frac{1}{2^n \sqrt{\pi}\, t^{\frac{n+1}{2}}} e^{-\frac{a^2}{4t}} He_n\left(\frac{a}{2\sqrt{t}}\right) = s^{\frac{n-1}{2}} e^{-a\sqrt{s}}$$

Key: The polynomials do not have exponential behavior.

A few examples are worked out for purposes of illustration.

In Eq. 1, Table I, form the exponents in the time domain

$$a(t,s) = -st - \frac{a^2}{4t} \; ; \quad a'(t,s) = 0 = -s + \frac{a^2}{4t^2} \; ; \quad \text{therefore } s = \frac{a^2}{4t^2} \quad .$$

Then form the exponents in the s domain

$$W(s,t) = st - a\sqrt{s} \; ; \quad W'(s,t) = 0 = t - \frac{a}{2\sqrt{s}} \; ; \quad \text{therefore } s = \frac{a^2}{4t} \quad .$$

In Eq. 2, Table I, form the exponents in the time domain

$$a(t,s) = -st - \frac{a^2}{4t} \; ; \quad \text{therefore } s = \frac{a^2}{4t^2} \quad .$$

Then form the exponents in the s domain

$$K_0(x) \text{ behaves as } e^{-x} \quad \text{then } st - a\sqrt{s} = W(s,t) \; ; \quad W'(s,t) = 0 = t - \frac{a}{2\sqrt{s}} \; ;$$

$$\text{therefore } s = \frac{a^2}{4t^2} \quad .$$

The key on each table gives the exponential behavior of the corresponding functions. With its use the correctness of the theorem can be verified throughout the entire table.

D. ACTIVE NETWORKS

Prof. E. A. Guillemin
Prof. J. G. Linvill
Dr. M. V. Cerrillo
J. G. Truxal

1. Broadband Amplifiers

The design procedure for broadband amplifiers with prescribed frequency characteristics described in earlier progress reports applies a new solution of the approximation problem of network synthesis. This solution to the approximation problem has a number of unique features which are useful in a broad range of synthesis problems. The rational approximating function obtained can be made to approximate both magnitude and phase characteristics which are prescribed over fractions of the whole frequency spectrum. The method of solution is one of successively improved trials, each trial solution possessing the same number of poles and zeros. The method is essentially one of determining the most desirable approximating function of a

predetermined complexity. The whole procedure is extremely flexible in that it permits one to apply constraints in the form of function to be obtained. For instance, one could constrain poles and zeros to lie at least a prescribed minimum distance from the imaginary axis of the complex frequency plane to insure that the network elements required need not be absolutely lossless.

Further illustrative examples are being worked and a technical report is in preparation which presents the approximation procedure.

J. G. Linvill

2. The Synthesis of Servomechanisms

The aim of this research is the development of a direct method for the synthesis of servomechanisms. This method proceeds from a determination of an overall system function directly from the specifications, with the result that such characteristics of the final design as bandwidth, relative stability, velocity constant and acceleration constant are predetermined. Working from this specification of the overall system function and from the known characteristics of the fixed part of the servomechanism, the appropriate compensation networks are derived.

Under the restrictive assumption that all components of the servomechanism are linear, the method of synthesis is straightforward. The stability of the overall system is governed principally by the location of the poles of the system function. To assure satisfactory stability, the poles of the overall system function are, at the outset of the design, placed in positions approximately as indicated in Fig. VIII-17. The two poles which govern both the bandwidth and the transient response are the conjugate poles a and b. All other poles are made to contribute negligibly to the bandwidth and to the general form of the transient response by either of two methods: they are placed well out into the left of the λ-plane near the real axis (poles marked c and d in the diagram), or they are placed adjacent to a zero (pole marked e in the diagram).

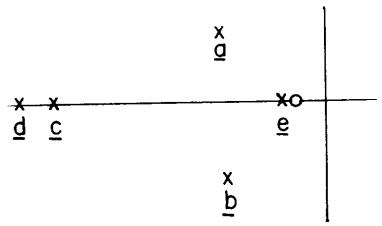

Fig. VIII-17 Possible positions of poles and zeros.

The exact location of the two principal poles is determined from the specifications of bandwidth and damping. The location of the zeros and the secondary poles is determined by the specifications of the velocity and acceleration constants. For example, an infinite velocity constant (corresponding to a zero-velocity-error servomechanism) demands a saddle-point in

the overall system function at the origin of the λ-plane. Various possible configurations for the poles and zeros yielding this saddle-point are shown below (Fig. VIII-18). The difference between the number of poles and the

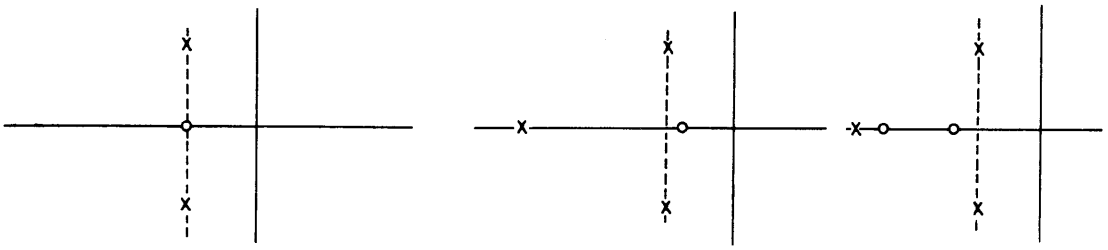

Fig. VIII-18 Possible configurations of poles and zeros to give saddle-point at origin.

number of zeros of the overall system function must equal the same quantity for the given, fixed part of the system in a practical design, as will be explained further in a forthcoming more detailed report.

Once the system function is determined, the only problem remaining is the determination of the compensation networks. The analytical relationships for a simple, single-loop servomechanism, as shown diagrammatically in Fig. VIII-19 are:

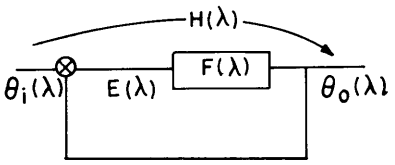

Fig. VIII-19
A simple, single-loop servomechanism.

$$H \equiv \frac{\theta_o(\lambda)}{\theta_i(\lambda)}$$

$$H(\lambda) = \frac{F(\lambda)}{1 + F(\lambda)} = \frac{p(\lambda)}{p(\lambda) + q(\lambda)}$$

where $p(\lambda)$ and $q(\lambda)$ are polynomials in λ.

$$F(\lambda) = \frac{p(\lambda)}{q(\lambda)} \quad .$$

The determination of the overall system function fixes both $p(\lambda)$ and $\left[p(\lambda) + q(\lambda)\right]$. The synthesis of the compensating network requires a determination of the roots of $q(\lambda)$. This determination can be made analytically, but it is probably more readily done graphically. If $\left[p(\lambda) + q(\lambda)\right]$ is evaluated for $\lambda = \sigma$ and plotted vs. the real variable σ, it will have the general form shown in Fig. VIII-20. In the simple case where $p(\lambda)$ is a constant, the real roots of $q(\lambda)$ are readily determined (as indicated by the points q_1 and q_2 on the diagram). If the compensating network is to be realizable as a passive RC transfer function, it must have only negative real poles, so that this graphical

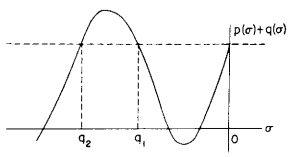

Fig. VIII-20 Form of $\left[p(\sigma) + q(\sigma)\right]$.

determination of the roots of $q(\lambda)$ will always work.

Although the above explanation relates only to the simple, single-loop servomechanism with unity feedback, the methods are readily extended to systems employing tachometric compensation in cases where the compensation network is more simply inserted around the fixed part of the system.

The major difficulties of any method of servomechanism synthesis seem to arise from two sources – non-linearity of the system components and the presence of unwanted disturbances. All of the above discussion is made under the stated assumption that the system is linear, but this assumed linearity is never realized in practice. Electrical motors are not linear, even though the flux density may be kept well below the saturation level. In addition to the non-linearity inherent in electrical motors, other non-linearities arise from variation in external conditions (for example, the change in the characteristics of a hydraulic transmission due to variation in the oil temperature). The second principal source of difficulty comes from the presence of unwanted signals. Noise and load torque disturbances are perhaps the commonest examples.

Both of these difficulties demand that any satisfactory synthesis procedure for servomechanisms include techniques for minimization of the sensitivity of the overall system function to changes in system parameters. It must at least be possible to keep these sensitivities below prescribed minimum values. The research is at the present time leading toward an investigation of this problem. E. A. Guillemin, J. G. Truxal

E. LOCKING PHENOMENA IN MICROWAVE OSCILLATORS

Prof. J. B. Wiesner
E. E. David, Jr.
W. P. Schneider

1. Theory

The mutual synchronization of two or more similar oscillators is being investigated in detail. The Rieke diagram and reflection-coefficient plane are currently being used in the investigation.

Approximate and differential analyser solutions to the Van der Pol equation are being considered. The equation is modified so as to describe an oscillator perturbed by an injected current.

2. Experimental Work

Experimental work is continuing in an effort to verify the theory presented in Part II of R.L.E. Technical Report No. 100.

Investigations are being carried out as to the feasibility of using locked oscillators for the transmission of information.

* * *